
Tracing α -element Abundances in the Milky Way using the GALAH Survey

Author:

Avidaan SRIVASTAVA

Department of Astronomy, Observatoire Astronomique de l'Université de Genève

Supervisors:

Sviatoslav BORISOV, Prof. Corinne CHARBONNEL

Thesis for Astrophysics Lab 2

Date: 1 May, 2023

Tracing α -element Abundances in the Milky Way using the GALAH Survey

Author:

Avidaan SRIVASTAVA (Department of Astronomy, Observatoire Astronomique de l'Université de Genève)

Supervisors:

Sviatoslav BORISOV, Prof. Corinne CHARBONNEL

Abstract

The primary objective of this project is to categorize the stars of the Milky Way galaxy based on their chemical and kinematic properties to better understand the chemical evolution of the galaxy as a whole. The main observations for this study are taken from the latest GALAH and Gaia data releases. The technique of Galactic Archaeology is used to investigate the final sample of 208,920 stars and sort them depending on if they belong in the thin disk or the thick disk of the Milky Way. The thin disk is primarily composed with Pop I stars that are younger, deficient in α -elements (chemical criterion) and have lower average kinetic energy (kinematic criterion). Thick disk stars on the other hand are mainly Pop II, rich in α -elements and have high average kinetic energy. Using the two independent ways of separation (chemical and kinematic), the resulting trends in α -elements gradient were compared which came out to be: stars of the thin disk were indeed on average α -poor than the stars of the thick disk. Additionally, a downward trend was observed which suggests that the α -rich stars are presents towards the galactic center and the α -poor stars are further out. Further analysis on the birth radii of the stars in the sample point to α -rich stars being produced far away from the galactic center. A proposed explanation for this occurrence is the inward migration of these stars via long term weak interactions with other stars and bodies.

Contents

Abstract	iii
1 Introduction	1
1.1 Galactic Archaeology	1
1.2 α -elements in stars	2
1.3 Division of Milky Way stars	2
2 Target Selection	5
2.1 Target Selection Criteria	5
2.1.1 NAN Entries and Errors	5
2.1.2 GAIA Astrometry	5
2.1.3 Stellar Parameters Filter	6
2.1.4 α -Element Abundance filter	6
2.1.5 Metallicity filter	6
2.1.6 Signal to Noise	6
3 Analysis	7
3.1 Radial Distribution of α -Elements in Milky Way	7
3.2 Division of stars in the Milky Way	10
3.2.1 Chemical Method	10
3.2.2 Kinematic Method	10
3.2.3 Similarities	13
3.3 Birth Radius	13
4 Conclusions	17
A Graphs	21

Chapter 1

Introduction

1.1 Galactic Archaeology

Stars go through several complex phases of changing internal conditions during their entire lifetime. The duration and nature of these phases may change depending on some initial parameters established during the formation of stars. The two major criteria that determine the direction of evolution in a star are its mass and metallicity.

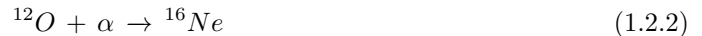
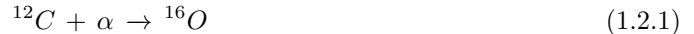
During the majority of the lifetime of a star it is usually not the radius, but its mass that stays conserved, hence the initial mass of the star determines its path of evolution [3]. Some stellar parameters that depend on its mass include, the duration of the main sequence phase, variation of central density and core temperature, and the luminosity of the star. Due to this central density and temperature dependence, the mass also governs what nuclear processes occur in the star and the kind of stellar remnant that it will give rise to at the end of its lifetime.

Metallicity, more importantly, gives us insight of the ongoing chemistry inside stars. Through spectroscopic analysis, it was discovered that the old Population II stars have a lower relative abundance of metals with respect to hydrogen, hence have a low metallicity [2]. The reason for this observation could be that, they evolve very slowly and take a long time to burn hydrogen. The newer stars (Population I) are born from the interstellar medium that has been enriched in metals that formed in the interiors of Population II stars. Hence, the relative abundances of metals in stars is an effective way to map out stellar evolution and formation, especially in the Milky Way. The abundances of various chemical species in a star's atmosphere also remain conserved since birth [10] which makes tracing of metallicity an effective way to study the evolution of stars. This type of study is known as Galactic Archaeology [9].

To further the study of stars via chemical analysis, the GALactic Archaeology with HERMES (GALAH) collaboration [7] was established, with its main observation period beginning in 2014. All the data for this survey is taken via the high resolution HERMES spectrograph located on the 3.9-m Anglo-Australian telescope. HERMES is capable of recording the spectra of around 400 stars simultaneously and at the time of writing this, the GALAH survey has accumulated 678,423 spectra from 588,571 stars. For the purposes of this project, data from the latest data release, GALAH+DR3 [9], was used along with some supplementary information from Gaia's latest observations, Gaia DR3 [10].

1.2 α -elements in stars

Nuclear fusion is the primary source of energy of a star and is responsible for producing a large majority of elements we observe in nature that have an atomic number higher than that of Helium. The high temperature and pressure conditions in the interior of stars facilitate this nuclear fusion and the resulting elements depend on the initial mass of the star and its stage of evolution. The alpha-process [1] is one way to produce new elements via the capture of alpha particles (He^{++}). An alpha chain is created such that each subsequent element in the chain is created by capturing an alpha particle Equation 3.1.1. The most common elements found in stars produced through this process are C^{12} , O^{16} , Ne^{20} , Mg^{24} , Si^{28} , S^{32} , Ar^{36} , Ca^{40} and Ti^{44} . Since very specific conditions are required to produce these alpha elements, measuring their abundance in stars can help acquire information regarding their age and more importantly, origin. Previous studies (Relative roles of type I and II supernovae in the chemical enrichment of the interstellar gas, 1986) have shown that the main source of α -element enrichment of the interstellar medium (ISM) are Type II supernovae (SNe) from the death of massive stars. Simultaneously, the increase in Type-Ia SNe over time increased the metallicity (Fe abundance) of the ISM. The GALAH survey reports the average α -abundance of a star using the mean abundances of O, Ne, Mg, Si, S, Ar, Ca and Ti.



so on... (1.2.3)

1.3 Division of Milky Way stars

Spectral analysis of the abundance of metals has revealed that there are some significant differences in the composition of stars in the Thin and Thick disk. The most likely cause of this difference is that both groups of stars were formed in interstellar media of different compositions. A Tinsley-Wallerstein diagram [9] (Figure 1.1) gives a better representation of this division. The higher density region, characterized by relatively higher metallicity ([Fe/H]) and relatively lower alpha element abundance ([α /Fe]) represents the stars of the thin disk [5], whereas the other population cloud with fewer stars in numbers and lower metallicity but higher alpha elements abundance are the stars of the thick disk. There is a third division of stars characterized by [Fe/H] < -1 which are the combined stars of the Galactic Bulge and the Halo.

Aside from chemical composition, the kinematics of the thin and thick disk stars also differ significantly [6]. Thin disk stars tend to have lower kinetic energy [4] while those of the thick disk have slightly higher kinetic energy. However, it is cautioned that such assumptions are most valid for the solar neighbourhood and if applied to the entire population of stars in the Milky Way can lead to miscategorization of stars close to the galactic center and those very far away from it. A comparative study of these two methods is therefore warranted to better understand what stars in the dataset actually belong to the thick or thin disks, to deduce their origin and history.

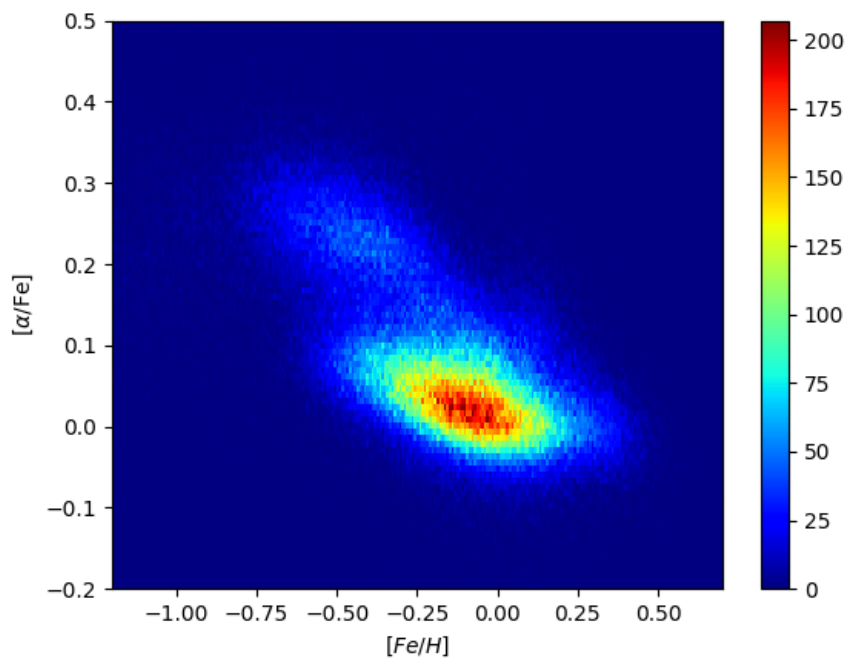


Figure 1.1: Tinsley-Wallerstein diagram for the final sample

Chapter 2

Target Selection

2.1 Target Selection Criteria

As mentioned previously, our data set is composed of GALAH+ DR3 with additional parameters for its stars gathered from the Gaia archive. Unfortunately, not all 588,484 stars had accurate measurements of all relevant parameters, which is why some stars needed to be filtered out to make sure our analysis of the sample would be more accurate. The GALAH+ DR3 came with 'quality flags' that can be used for the exact purpose for filtering out candidate stars that either lack, have incomplete, or inaccurate measurements of desired parameters. There are three primary quality flags we used, sequentially, and analyzed the sample after each filter was applied to accurately view their impacts. The filters used, in order, were: 'flag_sp', 'flag_alpha_fe' and 'flag_fe_h'. Additionally, we also decided to only accept the stars that had a $\text{SNR} > 30$ and had Gaia's resolution of single sources ('ruwe') value less than 1.4.

2.1.1 NAN Entries and Errors

Because of the large GALAH+ DR3 dataset, it was important to discard any stars that might have incomplete catalogued information for the relevant stellar properties that this project aims to analyze. Therefore, our very first data filter removed any 'nan' values for $[\alpha/\text{Fe}]$, $[\text{Fe}/\text{H}]$, galactic coordinates, distance of the star from the sun, all three components of stellar velocities and stellar age.

Due to the nature of our analysis, very precise measurements of $[\alpha/\text{Fe}]$ were needed. The median error for $[\alpha/\text{Fe}]$ for the stars in the GALAH data came out to be 0.048, going as high as 0.3 and as low as 0.01. For simplicity, all the stars that have $[\alpha/\text{Fe}]$ errors of greater than 0.05 were excluded from our final sample.

2.1.2 GAIA Astrometry

Since GALAH+ DR3 also included some quality flags from GAIA DR3, we were able to utilize the 'ruwe' < 1.4 condition to only keep accurately tracked stars in our dataset. In addition to this, we also discarded any 'nan' values under the quality flag, which resulted in the remaining star count in the catalogue to drop to 259,222.

2.1.3 Stellar Parameters Filter

Based on the quality flag 'flag_sp', we discarded all the stars who's value was anything but zero [9]. The number of stars left in the catalogue after applying this filter were 235,752.

2.1.4 α -Element Abundance filter

Similar to the stellar parameters filter, we only included stars for our analysis that had a 'flag_alpha_fe' of zero. However, the number of stars after applying this filter stayed at the same number (235,752) implying that the the nan-check and stellar parameters filter already discarded the unwanted candidates.

2.1.5 Metallicity filter

As with the previous two quality filters, the stars that passed the metallicity filter had the 'flag_fe_h' of zero. Only 87 stars failed this check, which left the 235,665 to move on to the final filter check.

2.1.6 Signal to Noise

Signal to Noise ratio is an important quantity to gauge if the data is good enough to use. Here, we only considered candidates with $\text{SNR} > 30$ so that a large majority of stars is still retained in our catalogue and the quality of data we have for these stars is sufficient for our analysis. In the end we wer left with the final sample size of 208,920 stars.

Chapter 3

Analysis

3.1 Radial Distribution of α -Elements in Milky Way

Since the primary objective of this project is to map out the abundance of alpha elements in the Milky Way and study their distribution, it is more useful to have the stellar distances relative to the galactic center instead of the sun. Equation 3.1.1 converts the sun-star distance (d_*) in the GALAH+ DR3 to Galactic Center (GC)-Star distance (d_{GC}). Here l and b are the galactic coordinates.

$$d_{GC} = \sqrt{d_*^2 + R_\odot^2 - 2 R_\odot d_* (\cos b) (\cos l)} \quad (3.1.1)$$

Figure 3.1 shows the radial profile of the Milky Way where the plane of the galaxy was divided into bins of size 0.1 kpc and the color gradient represents the number of stars in each of these bins. The dip in $[\alpha/\text{Fe}]$ at approximately the solar radius (8.2 kpc) is to be noted. There is also a sudden increase in the number of stars in the bins close to the solar radius due to the selection bias of the GALAH survey. In our sample 60.89 % of stars were within 1kpc of the Sun and 26.13 % within 500pc.

As we move further from the galactic center, there is a significant drop in the number of stars in each bin and beyond 13kpc there is no identifiable trend for $[\alpha/\text{Fe}]$. To better study this pattern, Figure 3.2 divides the radial profile showcasing the trends within 13kpc and beyond 13kpc. It is to be noted that the bin sizes for Figure 3.2(b) have been increased to 1pc to account for the sparse population of stars. Figure 3.3 further zooms in to observe the pattern near the solar radius to avoid any bias that may have appeared due to too many stars being grouped into a bin. However, the drastic decrease in $[\alpha/\text{Fe}]$ still persists.

The cause of this feature can be narrowed down to GALAH survey's selection bias. Figure 3.4 shows the radial and vertical distribution of the stars with the color-scale showing the different $[\alpha/\text{Fe}]$ values. Clearly seen here is a gap in the sample of stars that should be close to the galactic plane, near the center of the galaxy. The presence of the galactic bulge and the heavy dust extinction prevented data to be taken from stars that should be present there. So, the stars α -rich stars that would have been there were just not observed.

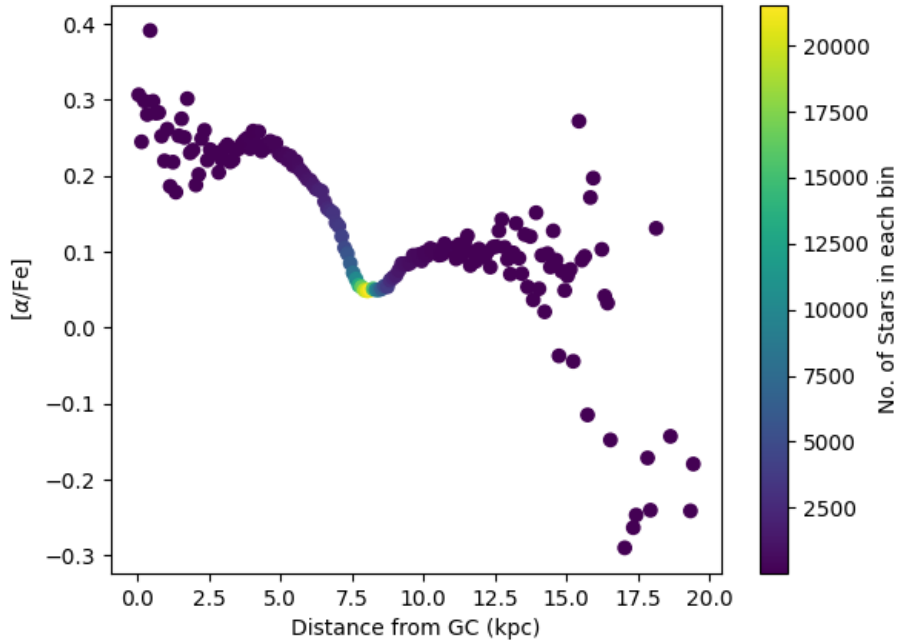


Figure 3.1: Binned gradient of alpha elements of all stars in the sample

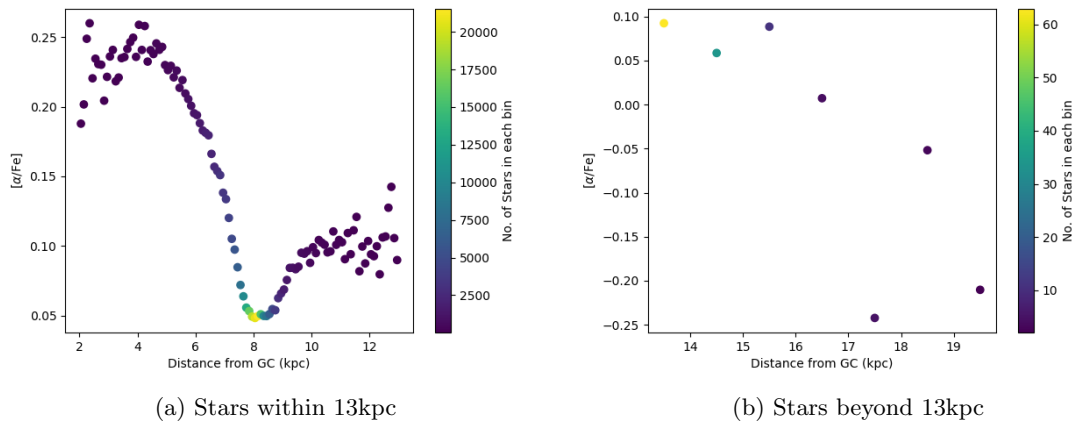


Figure 3.2: Binned alpha gradient of all stars within and beyond 13kpc boundary

3.1. RADIAL DISTRIBUTION OF α -ELEMENTS IN MILKY WAY

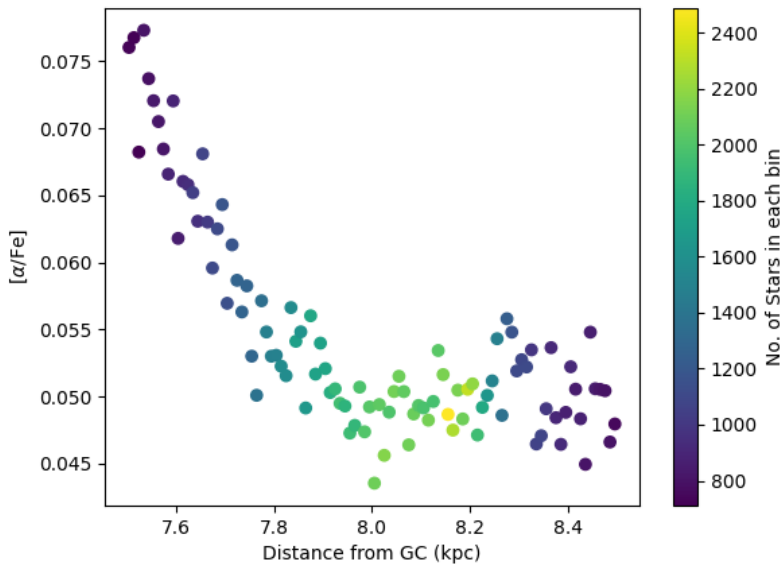


Figure 3.3: Zoomed in binned gradient of alpha elements near the sun's position

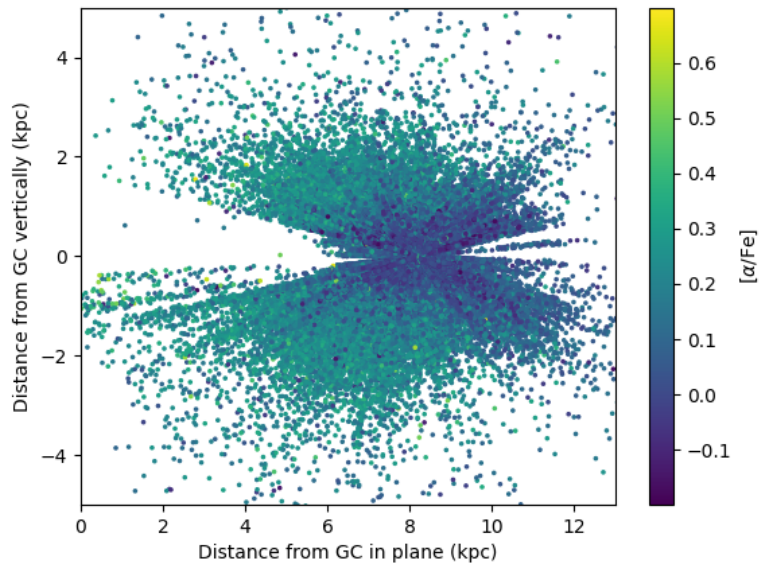


Figure 3.4: Distribution of the stars within 13kpc

3.2 Division of stars in the Milky Way

Based on their chemical and kinematic properties, stars in the Milky Way can be separated based on what part of the galaxy they belong to, the Thin Disk, the Thick Disk or the Bulge + Halo. As mentioned previously, there are two possible ways to divide the stars, chemically [5] and kinematically [6]. In this section, we attempted to study in detail the consistencies and inconsistencies between the two methods and how well their results agree with each other.

3.2.1 Chemical Method

To chemically distinguish the stars of the thin disk, thick disk and the combined bulge and halo, the Tinsley-Wallerstein density plot is used (Figure 1.1) that shows $[\alpha/\text{Fe}]$ plotted against $[\text{Fe}/\text{H}]$. The colour gradient here depicts the number of stars in each bin. Here there are two population clouds, one with significantly more stars having a higher metallicity content and lower α -element abundance than the other with higher $[\alpha/\text{Fe}]$ and lower $[\text{Fe}/\text{H}]$. Previous research has shown that the first criterion relates to stars of the thin disk while the latter to those of the thick disk. For the stars belonging to the bulge and halo, they are mainly identified by their extremely low metallicity ($[\text{Fe}/\text{H}] < -1$) and hence can be separated easily.

The remaining stars either belong to the thin or the thick disk, depending on which population cloud they correspond to. To statistically separate them, we divided the $[\text{Fe}/\text{H}]$ range of (-1, 0.5) into four bins with the following ranges: (-1, -0.5), (-0.5, -0.4), (-0.4, -0.2), (-0.2, 1). These ranges were specifically selected to have sufficient number of stars in them so as to not skew the results in any way while also keeping in mind the metallicity spreads of the two clouds in the Tinsley-Wallerstein diagram. The stars in each bins were then plotted in a histogram as shown in Figure 3.5 and a double gaussian was fit over both peaks. Each peak refers to the thin and thick disk star distribution and the intersection of the two gaussians can be assumed to be the point of division between the stars of the two disks. Figure 3.6(a) shows the same Tinsley-Wallerstein diagram but this time there is a red line over plotted which corresponds to the intersections of the gaussians of each bin and thus divides the stars of the thin (below the line) and thick (above the line) disks.

The size of the final bin is fairly large due to the stars of the thick disk decreasing significantly at $[\text{Fe}/\text{H}]$ of -0.2 and higher. However, the results can be improved upon by having our line of division trace the edge of the thin disk cloud. To do this, we further divided the $[\text{Fe}/\text{H}]$ range of (0, 0.6) into three equal bins of sizes 0.2 and statistically segregated the stars of each bin by making sure 20% of the stars remained above the line and 80% below. Figure 3.6(b) shows both the original and improved separation line on the Tinsley-Wallerstein diagram.

Out of the 208,920 stars, 154,965 were sorted to be a part of the thin disk, 51,321 belonged to the thick disk and the remaining 2,634 were considered to be a part of the combined bulge and halo. Figure 3.7 shows the binned radial profiles of the thin and thick disk stars separated by vertical distance bins.

3.2.2 Kinematic Method

The second way of separating stars is by analyzing their kinematic properties. The Gaia archive contains information on the kinematics of the stars relative to the solar cluster. The velocity v corresponds to the velocity in the direction of rotation of the Milky Way, u for the direction towards the galactic center and w refers to the velocity component perpendicular to the galactic plane. The distribution shown in Figure 3.8(a) plots v versus the net velocity, also known as the

3.2. DIVISION OF STARS IN THE MILKY WAY

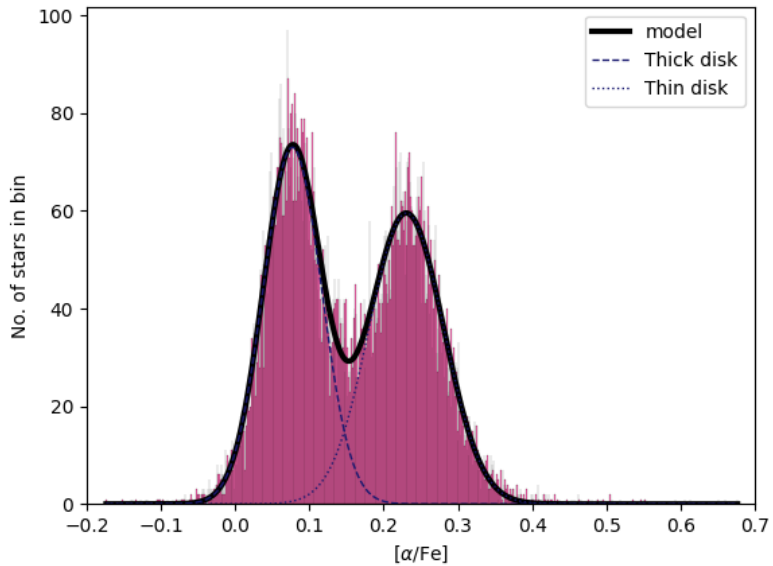


Figure 3.5: Distribution of stars in the metallicity range: -0.5, -0.4

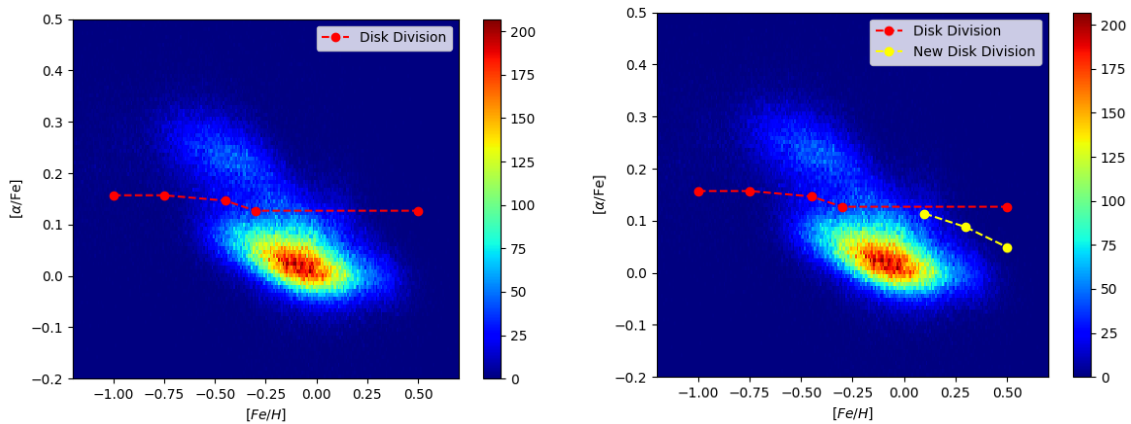


Figure 3.6: Tinsley-Wallerstein diagram with thin and thick disk stars separated

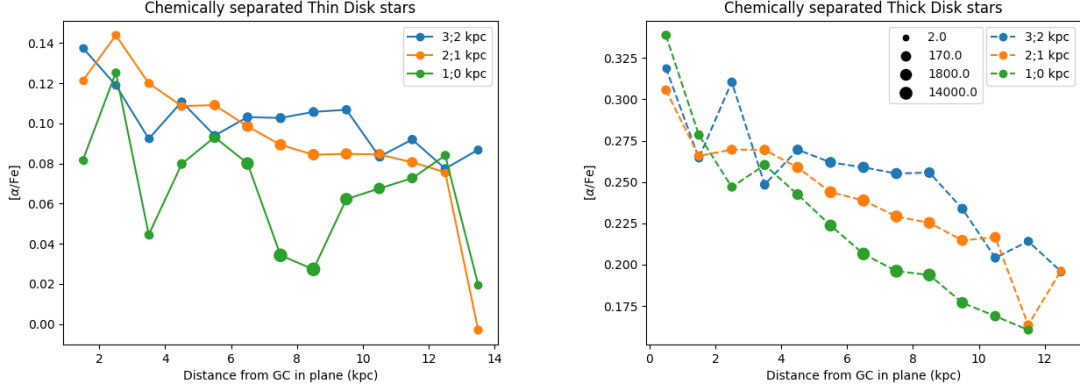
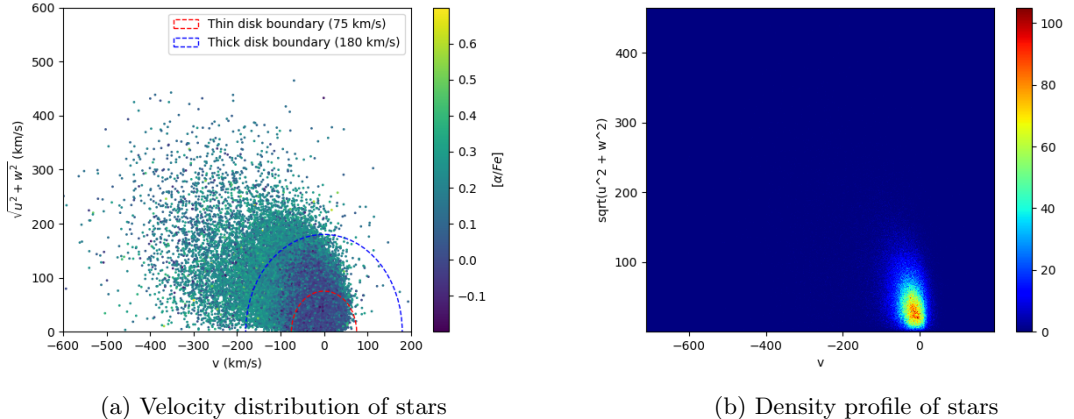


Figure 3.7: Radial distribution of stars in the thin and thick disk relative to their position with respect to the galactic plane

Toomre diagram. The striking feature about this graph is that there are a lot of stars that have a negative value for v , meaning that the Sun moves faster than an average star in the Milky Way in the galaxy's rotational direction.



(a) Velocity distribution of stars

(b) Density profile of stars

Figure 3.8: Toomre diagram showing the kinematics of all the stars in the sample

Results from another paper [6] show that if semicircle arcs of radii 75-km/s and 180-km/s are over plotted, the thin disk stars would be those within the 75-km/s circle, the thick disk stars between the 75-km/s and 180-km/s radii and the ones beyond the 180-km/s radius are the remnants corresponding to the bulge and halo stars. Figure 3.8(b) also depicts a density plot of this velocity distribution and it can be clearly seen that the majority of stars lie within our designated region for thin disk stars, which aligns with real world observations.

3.2.3 Similarities

Now that the two methods have been tackled, we compared their results. Theoretically, the stars sorted in the thin disk, thick disk or bulge-halo categories by both methods should be the same. However, Table 1 displays the results of our comparison. While the majority of thin and thick disk star sorting was consistent between the two methods, percentage-wise there is a large disparity in the bulge-halo stars, which could also be a result of our selection bias that the sample size of stars belonging to that part of the galaxy itself is quite low.

Part of MW	No. of stars from Chemical method	No. of stars from Kinetic method	No. of common stars
Thin Disk	154965	137993	120390
Thick Disk	51321	63773	29448
Bulge + Halo	2634	7154	1887
Total	208920		

Table 1: Table showing the distribution of stars in each category depending on the method of separation

Figure 3.2 also shows the comparison between the chemically and kinematically separated thin and thick disk stars. Both methods show a downwards trend in the α -abundance, i.e., α -rich stars are present mainly in the inner parts of the galaxy and the α -poor stars in the outer regions. The chemical method shows a clear distinction between the thin and thick disk gradients which is to be expected as the α -abundance was the factor used to separate the two. The kinematic method on the other hand has a much more mixed gradient for both the disks. However, if each vertical bin is observed more closely, on average the thick disk gradient shows a higher α -abundance compared to the thin disk. Therefore, the results from the two methods of separation do agree to some capacity, just not globally.

3.3 Birth Radius

Another quantity that we were able to deduce was the birth radii of all the stars in the final sample using the stars' ages and metallicity and relating them to the evolution of metallicity of the ISM in the Milky Way [8]. Figure 3.3 shows the results of the aforementioned study reproduced and Equation 3.3.1 relates them to the birth radius of the star.

$$R_{birth} = \frac{[Fe/H]_* - [Fe/H]_{R_{\odot},t}}{\nabla[Fe/H]_{ISM}} + R_{\odot} \quad (3.3.1)$$

Figure 3.4 has the calculated birth radii of stars plotted against the guiding radius of each star, the average of the apoapse and periapse radius. The selection bias of the GALAH survey is once again amplified here where the guiding radius for most stars is around the solar radius. The birth radii on the other hand show quite a large spread. Plotting the colourscale as the age of the star, it is to be noted that most of the old stars were born quite far away from the galactic center (15 kpc+ away). These stars would therefore be of the Population II (α -rich) category and would constitute mainly the thick disk. This trend (Figure 3.5) suggests that these old stars migrated inwards over

CHAPTER 3. ANALYSIS

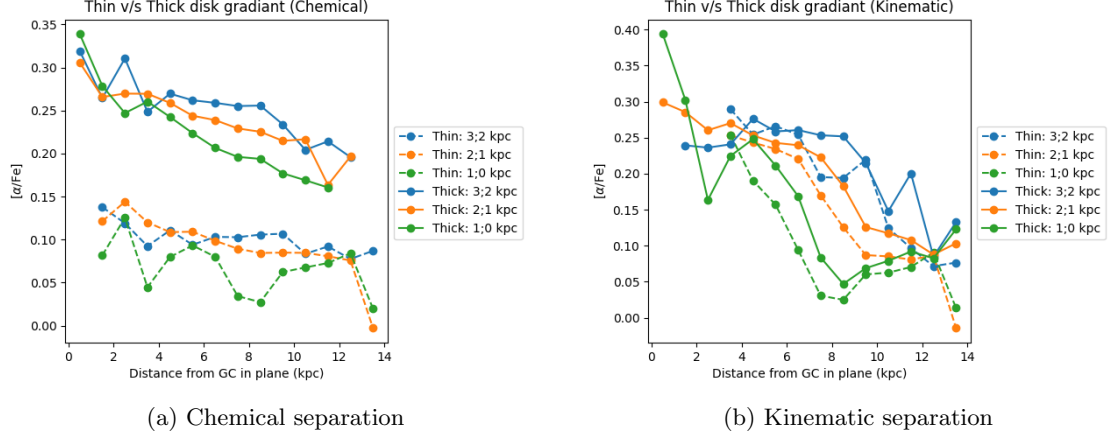


Figure 3.2: Comparison between the radial profiles of thin and thick disk stars separated using the two different methods

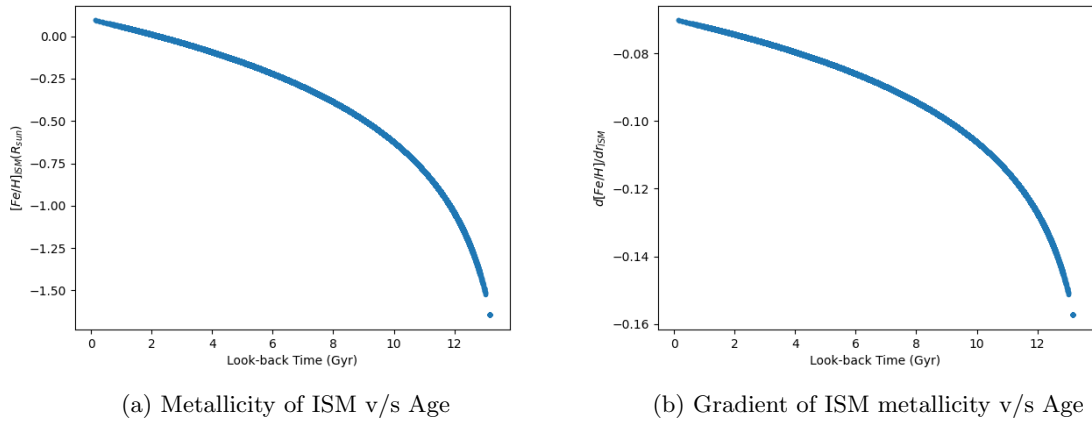


Figure 3.3: Results from a previous study [8] reproduced, which were used in the calculation of birth radii of stars

3.3. BIRTH RADIUS

time and increased the α -abundance towards the galactic center. One possible explanation for this migration could be that since these stars are older, they have had much more time to 'weakly-interact' with other stars in the galaxy and exchange energy, slowly moving towards the center. This is also supported by the fact that the thick disk stars have higher kinetic energies (Toomre diagram), due to the many interactions they have had.

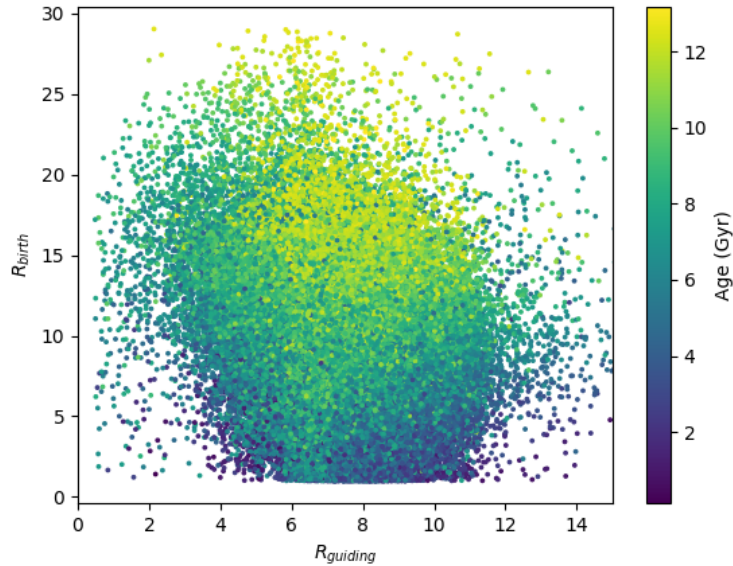


Figure 3.4: Statistical relation between the birth radius and guiding radius with age of the star as the colour gradient

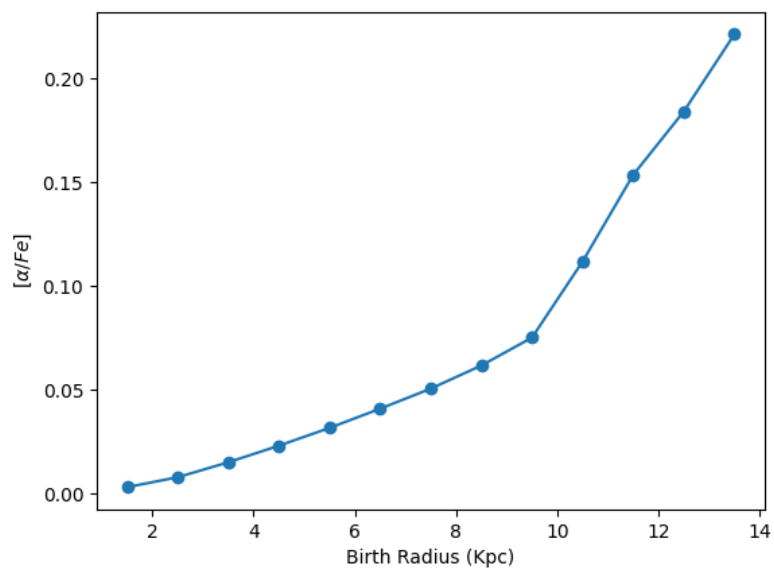


Figure 3.5: Radial distribution of α -abundance of stars with respect to their birth radius

Chapter 4

Conclusions

This research project on the topic of Galactic Archaeology used observational data from the latest data releases from both the GALAH survey (GALAH+ DR3) and Gaia (Gaia DR3) to study the dichotomy of stars in the Milky Way galaxy. The younger (Population I), metal rich, α -poor stars generally constitute the so called Thin disk, whereas the older (Population II), metal-poor, α -rich stars make up the Thick disk. The 588,464 stars in the GALAH catalogue were first filtered by discarding 'nan' values, quality flags, astrometric solution, error limits and SNR constraints, leaving behind the final sample of 208,920 stars. A prominent selection effect is observed for these stars where there is a 'dip' in the $[\alpha/Fe]$ distribution around 8-kpc due to the lack of stars observed near the bulge that would flatten out the curve. The overall distribution of the stars is however consistent with the results from Gaia [10], despite the relatively low sample size (Figure 4.1).

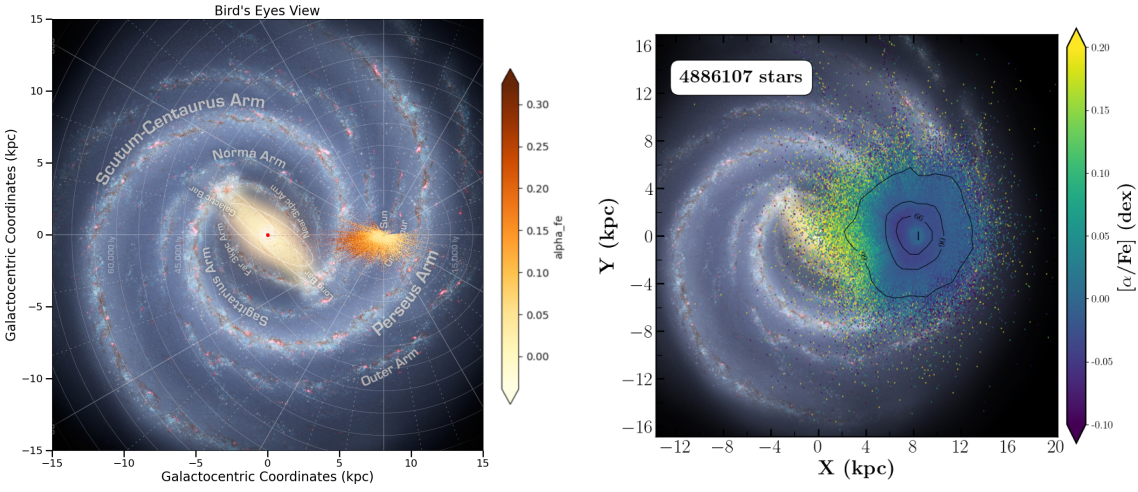


Figure 4.1: Comparison between the distribution of stars based on the α -abundance

CHAPTER 4. CONCLUSIONS

These stars were separated into the thin and thick disk categories using two different methods, based on their chemistry and kinematics. The chemical method used the aforementioned difference in α -element abundance of Pop I and II stars, whereas the kinematic method used the velocity distributions of the stars, with the Pop II stars having higher kinetic energy than Pop I stars. Comparing the $[\alpha/Fe]$ radial distributions of the thin and thick disks using both these methods led to the conclusion that the results agree in some capacity. Both indicate a downwards gradient of $[\alpha/Fe]$ with distance, pertaining to the galactic center being α -rich. The main difference lies in the fact that the thick disk stars are not always α -rich compared to the thin disk stars when separated kinematically, which was the basis for their chemical separation. However, close examination suggests that when the sample is divided into vertical distance bins, for each bin, the chemical and kinematic separation results match.

Further analysis involving the birth radii of these stars suggests a contradiction to the currently observed $[\alpha/Fe]$ gradient, where the α -rich stars were born far away from the galactic center, as opposed to the currently observed α -rich galactic center. One proposed explanation for this is the inward migration of these stars through large number of interactions with other stars.

Bibliography

- [1] E. Margaret Burbidge et al. “Synthesis of the Elements in Stars”. In: *Rev. Mod. Phys.* 29 (4 Oct. 1957), pp. 547–650. DOI: [10.1103/RevModPhys.29.547](https://doi.org/10.1103/RevModPhys.29.547). URL: <https://link.aps.org/doi/10.1103/RevModPhys.29.547>.
- [2] Page and Thornton. *The evolution of stars: how they form, age, and die*. Edited by Thornton Page Lou Williams Page. eng. Sky and telescope library of astronomy, v. 6. New York: Macmillan, 1967.
- [3] Salaris and Cassisi. *The Hydrogen Burning Phase*. John Wiley Sons, Ltd, 2005. Chap. 5, pp. 117–159. ISBN: 9780470033456. DOI: <https://doi.org/10.1002/0470033452.ch5>. eprint: <https://onlinelibrary.wiley.com/doi/pdf/10.1002/0470033452.ch5>. URL: <https://onlinelibrary.wiley.com/doi/abs/10.1002/0470033452.ch5>.
- [4] Bensby, T. et al. “Chemical evolution of the Galactic bulge as traced by microlensed dwarf and subgiant stars - IV. Two bulge populations”. In: *A&A* 533 (2011), A134. DOI: [10.1051/0004-6361/201117059](https://doi.org/10.1051/0004-6361/201117059). URL: <https://doi.org/10.1051/0004-6361/201117059>.
- [5] Miho N. Ishigaki, Masashi Chiba, and Wako Aoki. “CHEMICAL ABUNDANCES OF THE MILKY WAY THICK DISK AND STELLAR HALO. I. IMPLICATIONS OF [Fe/H] FOR STAR FORMATION HISTORIES IN THEIR PROGENITORS”. In: *The Astrophysical Journal* 753.1 (June 2012), p. 64. DOI: [10.1088/0004-637X/753/1/64](https://doi.org/10.1088/0004-637X/753/1/64). URL: <https://dx.doi.org/10.1088/0004-637X/753/1/64>.
- [6] Timothy C. Beers et al. “POPULATION STUDIES. XIII. A NEW ANALYSIS OF THE BIDELMAN-MACCONNELL “WEAK-METAL” STARS—CONFIRMATION OF METAL-POOR STARS IN THE THICK DISK OF THE GALAXY”. In: *The Astrophysical Journal* 794.1 (Sept. 2014), p. 58. DOI: [10.1088/0004-637X/794/1/58](https://doi.org/10.1088/0004-637X/794/1/58). URL: <https://dx.doi.org/10.1088/0004-637X/794/1/58>.
- [7] G. M. De Silva et al. “The GALAH survey: scientific motivation”. In: 449.3 (May 2015), pp. 2604–2617. DOI: [10.1093/mnras/stv327](https://doi.org/10.1093/mnras/stv327). arXiv: [1502.04767 \[astro-ph.GA\]](https://arxiv.org/abs/1502.04767).
- [8] I. Minchev et al. “Estimating stellar birth radii and the time evolution of Milky Way’s ISM metallicity gradient”. In: 481.2 (Dec. 2018), pp. 1645–1657. DOI: [10.1093/mnras/sty2033](https://doi.org/10.1093/mnras/sty2033). arXiv: [1804.06856 \[astro-ph.GA\]](https://arxiv.org/abs/1804.06856).
- [9] Sven Buder et al. “The GALAH+ survey: Third data release”. In: 506.1 (Sept. 2021), pp. 150–201. DOI: [10.1093/mnras/stab1242](https://doi.org/10.1093/mnras/stab1242). arXiv: [2011.02505 \[astro-ph.GA\]](https://arxiv.org/abs/2011.02505).
- [10] Gaia Collaboration et al. “Gaia Data Release 3 - Chemical cartography of the Milky Way”. In: *A&A* 674 (2023), A38. DOI: [10.1051/0004-6361/202243511](https://doi.org/10.1051/0004-6361/202243511). URL: <https://doi.org/10.1051/0004-6361/202243511>.

Appendix A

Graphs

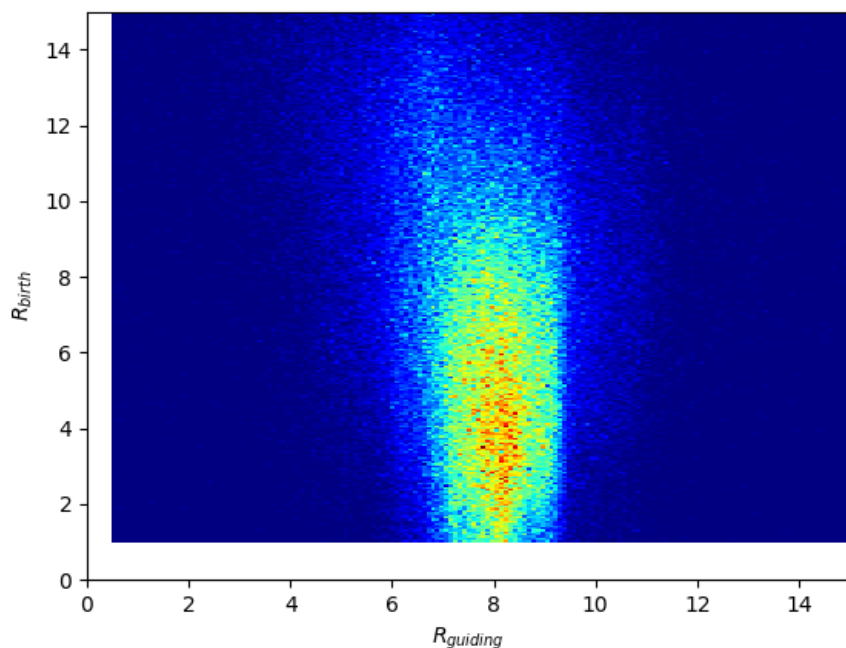


Figure A.1: Density plot featuring the guiding radii and birth radii of stars

APPENDIX A. GRAPHS

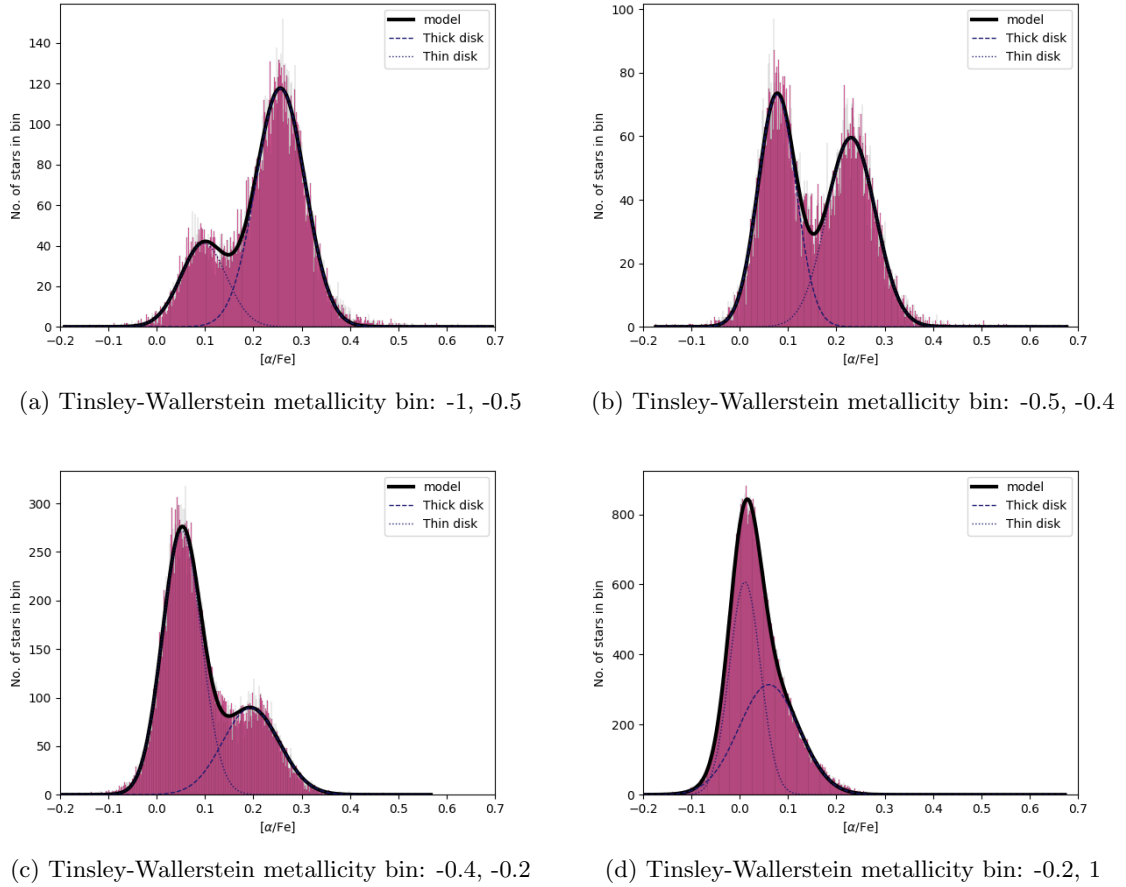
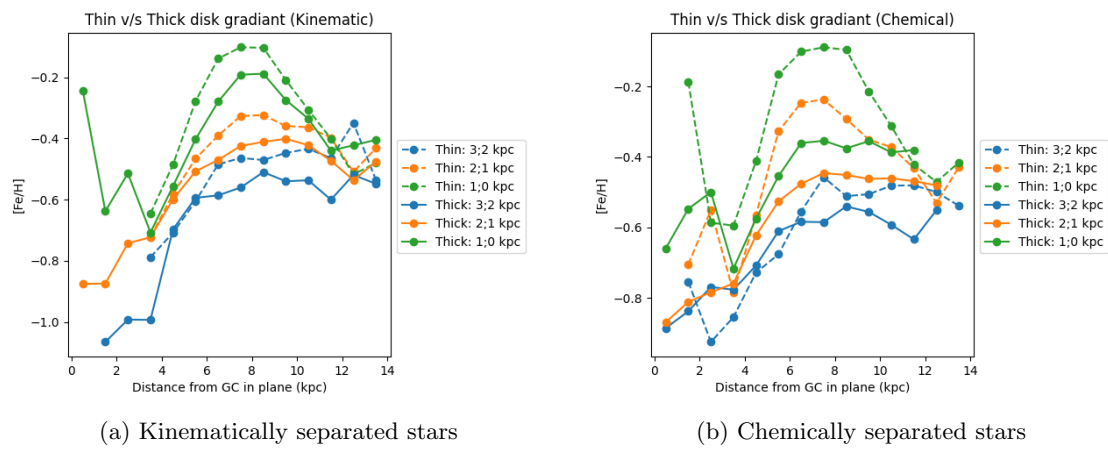


Figure A.2: Stars in each metallicity bin used to find the line of division between thin and thick disk stars in a Tinsley-Wallensteine diagram



(a) Kinematically separated stars

(b) Chemically separated stars

Figure A.3: Metallicity gradient comparison between the thick and thin disk stars separated using different methods